New Molecular Conductors Based on ETEDT−TTF Trihalides: From Single Crystals to Conducting Layers of Nanocrystals

ARTICLE *in* CHEMISTRY OF MATERIALS · AUGUST 2002

Impact Factor: 8.35 · DOI: 10.1021/cm021123g

17 AUTHORS, INCLUDING:

Elies Molins
Materials Science Institute of Barcelona
586 PUBLICATIONS **9,416** CITATIONS
SEE PROFILE

Jaume Veciana
Spanish National Research Council
981 PUBLICATIONS **12,167** CITATIONS
SEE PROFILE

Elena Laukhina
Spanish National Research Council
118 PUBLICATIONS **1,034** CITATIONS
SEE PROFILE

Concepcio. Rovira
Spanish National Research Council
528 PUBLICATIONS **8,950** CITATIONS
SEE PROFILE

New Molecular Conductors Based on ETEDT-TTF Trihalides: From Single Crystals to Conducting Layers of Nanocrystals

M. Mas-Torrent,[†] E. Ribera,[†] V. Tkacheva,[‡] I. Mata,[†] E. Molins,[†] J. Vidal-Gancedo,[†] S. Khasanov,[§] L. Zorina,[§] R. Shibaeva,[§] R. Wojciechowski,[∥] J. Ulanski,[∥] K. Wurst,[⊥] J. Veciana,[†] V. Laukhin,[†,‡,#] E. Canadell,[†] E. Laukhina,[†,‡] and C. Rovira*[,†]

Institut de Ciència de Materials de Barcelona, CSIC, Campus Univeritari de Bellaterra, E-08193 Cerdanyola, Spain, Institut of Problems of Chemical Physics and Institut of Solid State Physics, RAS, 142432, Chernogolovka, MD, Russia, Department of Molecular Physics, Technical University of Lodz, 90-924 Lodz, Poland, and Institute für Allgemeine Anorganische und Theoretische Chemie, Universität Innsbruck, Innrain 52a, A-6020 Innsbruck, Austria

Received January 22, 2002. Revised Manuscript Received April 3, 2002

Electrocrystallization of the novel π-electron donor (ethylenethio)(ethylenedithio)-tetrathiafulvalene (ETEDT-TTF) with trihalide anions has given rise to a new family of radical cation salts with insulating properties, [ETEDT-TTF]X, and conducting properties, ETEDT-TTF]$X_{0.42}$, where X = I_3^- or $I_yBr_{3-y}^-$. According to X-ray data, in the isostructural completely ionic [ETEDT-TTF]X salts, the donor radical cations are strongly dimerized, with an interplane distance of 3.310−3.317 Å, and the mixed-valence [ETEDT-TTF]$(I_3)_{0.42}$ salt is formed by segregated radical cation and anion layers alternating along the *b* axis. The latter salt exhibits semiconductor behavior with a high room-temperature conductivity of 24 S·cm^{-1}. The large angle between the molecular planes of the donors in neighboring stacks precludes the possible metallic behavior of this salt. Interestingly, nanocrystals of the mixed-valence salts are the conducting component of new bilayer (BL) composite films that have been generated via the ETEDT-TTF + I_2 and ETEDT-TTF + IBr chemical reactions. The structure and composition of the conducting layers of these new BL films were confirmed by X-ray, EPR, and Raman spectroscopies. Similarly to the single crystals, these composite materials exhibit semiconducting behavior with a room-temperature conductivity ranging from 0.25 to 2.5 S·cm^{-1}. SEM and NIR studies of the film samples were also carried out.

Introduction

Since the discovery of the first organic metal TTF-TCNQ in 1972,[1] the development of new π-electron donors based on tetrathiafulvalene and its analogues has remained at the forefront of research in the field of organic metals, resulting in a multitude of metals and superconductors. In the search for electron-donor molecules as sources for new organic superconductors, multichalcogen TTF derivatives have been the most successful choice. The main reason for this success is their ability to produce 2D electronic structures through S···S contacts while avoiding the observed structural changes that promote metal-to-insulator transitions in 1D conductors, and hence, allowing the transition to the superconducting state.[2] To date, the bis(ethylenedithio)-tetrathiafulvalene (BEDT-TTF) donor has provided the largest number of molecular superconductors[2b] and forms the salt with the highest known T_c, 12.8 K.[3]

Following this approach in the design of new organic conductors with external sulfur atoms, our group previously synthesized a new disymmetric donor ETEDT-TTF [(ethylenethio)(ethylenedithio)tetrathiafulvalene] that can be considered as a combination of one-half BEDT-TTF and one-half BET-TTF (Scheme 1).[4] The latter donor gives rise to a family of isostructural salts with octahedral counteranions XF_6^- (X = P, Sb, As) that exhibit stable metallic properties, and thus, it seems to be a good building block for the synthesis of organic

* Author for correspondence: Dr. C. Rovira,e-mail: cun@icmab.es. Address: Institut de Ciència de Materials de Barcelona, Campus UAB, E-08193 Bellaterra, Spain. Telephone: +34935801853. Fax: +34935805729.
† Institut de Ciència de Materials de Barcelona, CSIC.
‡ Institut of Problems of Chemical Physics, RAS.
§ Institut of Solid State Physics, RAS.
∥ Technical University of Lodz.
⊥ Universität Innsbruck.
Present affiliation: Institució Catalana de Recerca i Estudis Avançats (ICREA), Pg. Lluis Companys 23, 08010 Barcelona, Spain

(1) Ferraris, J.; Cowan, D. O.; Walatka, V. V.; Perlstein, J. H. *J. Am. Chem. Soc.* **1972**, *94*, 3372.
(2) (a) *The Physics and Chemistry of Organic Superconductor*; Saito, G., Kagoshima, S., Eds.; Springer: Berlin, 1990. (b) Organic Superconductor (Including Fullerenes). Synthesis, Structure, Properties and Theory; Williams, J. M., Ferraro, J. R., Thorn, R. J., Carlson, K. D., Geiser, U., Wang, A H. H., Kini, M., Whango, M.-H., Eds.; Prentice Hall: Upper Saddle River, NJ, 1992.
(3) Williams, J. M.; Kini, A. M.; Wang, H. H.; Carlson, K. D.; Geiser, U.; Montgomery, L. K.; Pyrca, G. J.; Watkins, D. M.; Kommers, J. M.; Boryschuk, S. J.; Crouch, A. V. S.; Kwok, W. K.; Schirber, J. E.; Overmyer, D. L.; Jung, D.; Whangbo, M.-H. *Inorg. Chem.* **1990**, *29*, 3262.
(4) Ribera, E.; Veciana, J.; Molins, E.; Mata, I.; Wurst, K.; Rovira, C. *Eur. J. Org. Chem.* **2000**, 2867.

10.1021/cm021123g CCC: $22.00
Published on Web 06/26/2002

Scheme 1

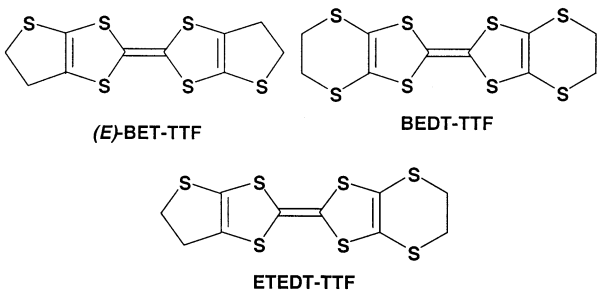

conductors offering good prospects for stable metals and even superconductors. These encouraging results prompted us to seek different anions able to promote salts with interesting transport properties. It is well-known that trihalide anions are promising counteranions for the preparation of novel molecular metals and superconductors based on cation-radical salts of organic donors. Indeed, the β-[BEDT-TTF]$_2$I$_3$ and β-[BEDT-TTF]$_2$IBr$_2$ salts exhibit superconductivity.[5] Additionally, the use of these anions for obtaining organic metals also offers the interesting possibility of preparing conducting bilayer composite films (BL films).[6] These films consist of polymeric matrixes with a conducting surface layer formed by a nanocrystalline network of organic conductors. One great advantage of this method of preparation is that it results in BL films that combine the unusual electronic properties of molecular metals (e.g., metallic conductivity, superconductivity) together with the favorable properties of a polymeric matrix (e.g., flexibility, transparency, low density).[7] Such films also overcome the known technological limitations of single crystals of organic conductors (e.g., low processability, quantity).

Herein, we report on the preparation of a new family of salts based on ETEDT-TTF and the trihalide anions, I_3^-, I_2Br^-, and IBr_2^-, which display a variety of properties ranging from semiconducting to insulating behavior. We also describe the preparation and characterization of BL films containing a thin layer of a nanocrystalline network generated from the chemical reactions ETEDT-TTF + I_2 and ETEDT-TTF + IBr. Interestingly, these new BL films exhibit the same physical properties as the mixed-valence single crystals.

Experimental Section

(Ethylenethio)(ethylenedithio)tetrathiafulvalene. (Ethylenethio)(ethylenedithio)tetrathiafulvalene was prepared as previously described.[4]

Preparation of Single Crystals. [ETEDT-TTF]$_x$I$_3$ and [ETEDT-TTF]$_x$(I$_y$Br$_{3-y}$) crystals were obtained by electrocrystallization from chlorobenzene (PhCl) or tetrahydrofuran (THF) solutions of the donor and the corresponding tetrabutylammonium salt as the electrolyte, in approximately stoichiometric amounts, with Pt electrodes and under galvanostatic conditions. The current was typically 1 μA. After 1 week of electrocrystallization, black ruler-shaped crystals were obtained.

Film Preparation. Polycarbonate films containing 2 wt % of molecularly dispersed ETEDT-TTF were cast as previously described.[8] As a second step, the surface of each casted PC/ETEDT-TTF film was treated with vapors of either a IBr/CH_2Cl_2 or a I_2/CH_2Cl_2 solution at equilibrium for different time periods, which resulted in the formation of a conducting surface layer with an interpenetrating network of [ETEDT-TTF]$_x$I$_3$ or [ETEDT-TTF]$_x$(I$_y$Br$_{3-y}$) nanocrystals. The mole fraction of IBr or I_2 contained in the solution was always much greater than the mole fraction of ETEDT-TTF contained in the swollen surface layer of the film. All time periods used for the film surface treatment were not sufficient to achieve saturation of the swollen layer of the film with IBr or I_2. The optimum conditions were found using solutions 0.03 M IBr and I_2 in CH_2Cl_2 and treatment time periods ranging from 1 to 3 min.

Characterization. *X-ray Crystal Structures.* For [ETEDT-TTF]I$_3$, single-crystal data were collected with an Enraf Nonius CAD4 diffractometer using monochromatic Mo Kα radiation (λ = 0.710 69 Å). The cell parameters were determined from a least-squares refinement of 25 reflections randomly searched. Data were collected by using an $\omega-2\theta$ scan method. The MolEN[9] package was used for applying Lorentz polarization and Ψ-scan empirical absorption corrections. The structures were solved by direct methods using SHELXS97[10] and refined by a full matrix least-squares method using SHELXL97.[11] The least-squares calculation minimized $\Sigma w(\Delta F)^2$, where $w = [\sigma^2(F_{02}) + (aP)^2 + bP]^{-1}$ and $P = (F_{02} + 2F_c^2)/3$. Non-H atoms were anisotropically refined, and H atoms were positioned in calculated positions and refined with a global isotropic temperature factor.

For [ETEDT-TTF](I$_3$)$_{0.42}$, X-ray *a*-axis-rotation photographs of these crystals exhibit two independent sets of layer lines: one consists of sharp Bragg diffraction spots, and the other has diffuse layer lines, with the common zero-layer line being composed of sharp reflections only. In accordance with this diffraction pattern, the assumption was made that the crystal was composed of two intergrowing sublattices: (1) an ETEDT-TTF donor sublattice that has long-range order and three-dimensional periodicity and (2) iodine chains, which are not firmly pinned relative to the donor sublattice; as a result, the chains have positional disorder along the *a* axis, so that this sublattice has no three-dimensional long-range order, although it does have two-dimensional periodicity in its (100) plane. The diffuse lines observed in the X-ray diffraction photographs

(5) (a) Yagubskii, E. B.; Shchegolev, I. F.; Laukhin, V. N.; Kononovich, P. A.; Kartsovnik, M. V.; Zvarykina, A. V.; Buravov, L. I. *Pis'ma v Zh. Eksp. Teor. Fiz.* **1984**, *39*, 12 (*JETP Lett.* **1984**, *39*, 12). (b) Williams, J. M.; Wang, H. H.; Beno, M. A.; Emge, T. J.; Sowa, L. M.; Copps, R. T.; Behroozi, F.; Hall, L. N.; Karlson, K. D.; Crabtree, G. W. *Inorg. Chem.* **1984**, *23*, 3839. (c) Yagubskii, E. B.; Shchegolev, I. F.; Shibaeva, R. P.; Fedutin, D. N.; Rozenberg, L. P.; Sogomonyan, E. M.; Lobkovskaya, R. M.; Laukhin, V. N.; Ignat'ev, A. A.; Zvarykina, A. V.; Buravov, L. I. *Pis'ma v Zh. Eksp. Teor. Fiz.* **1985**, *42*, 167 (*JETP Lett.* **1985**, *429*, 206). (d) Baran, G. O.; Buravov, L. I.; Degtyarev, L. S.; Kozlov, M. E.; Laukhin, V. N.; Laukhina, E. E.; Onishchenko, V. G.; Pokhodnya, K. I.; Sheinkman, M. K.; Shibaeva, R. P.; Yagubskii, E. B. *Pis'ma v Zh. Eksp. Teor. Fiz.* **1986**, *44*, *6*, 293 (*JETP Lett.* **1986**, *44*, 376). (e) Creuzet, F.; Creuzet, G.; Jerome, D.; Schweitzer, D.; Keller, H. J. *J. Phys. Lett.* **1985**, *46*, 1079. (f) Laukhina, E. E.; Laukhin, V. N.; Khomenko, A. G.; Yagubskii, E. B. *Synth. Met.* **1989**, *32*, 381.

(6) (a) Laukhina, E. E.; Merzhanov, V. A.; Pesotskii, S. I.; Khomenko, A. G.; Yagubskii, E. B.; Ulanski, J.; Kryszewski, M.; Jeszka, J. K. *Synth. Met.* **1995**, *70*, 797. (b) Laukhina, E. E.; Ulanski, J.; Khomenko, A. G.; Pesotskii, S. I.; Tkachev, V.; Atovmyan, L.; Yagubskii, E. B.; Rovira, C.; Veciana, J.; Vidal-Gancedo J.; Laukhin, V. *J. Phys. I Fr.* **1997,** *7*, 1665. (c) Horiuchi, S.; Yamochi, H.; Saito, G.; Jeszka, J. K.; Tracz, A.; Sroczyñska, A.; Ulanski, J. *Mol. Cryst. Liq. Cryst.* **1997**, *296*, 365. (d) Laukhina, E.; Tkacheva, V.; Shibaeva, R.; Khasanov, S.; Rovira, C.; Veciana, J.; Vidal-Gancedo, J.; Tracz, A.; Jeszka, J. K.; Sroczynska, A.; Wojciechowski, R.; Ulanski, J.; Laukhin, V. *Synth. Met.* **1999**, *102*, 1785.

(7) Mas-Torrent, M.; Laukhina, E.; Rovira, C.; Veciana, J.; Tkacheva, V.; Zorina, L.; Khasanov, S. *Adv. Funct. Mater.* **2001**, *11*, *4*, 299.

(8) (a)Ulanski, J.; Kryszewski, M. In *The Encyclopedia of Advanced Materials*; Bloor, D., Brook, R. J., Fleming, M. C., Mahajan, S., Cahn R. W., Eds.; Pergamon Press: Oxford, U.K., 1994, p 2301. (b) Ulanski, J.; Tracz, A.; Jeszka, J. K.; Laukhina, E.; Khomenko, A.; Polanowski, P.; Staerk D.; Helberg H. W. in *NATO ARW: Electrical and Related Properties of Organic Solids*; Munn, R. W., Kuchta, B., Miniewich, A., Eds.; Kluwer Academic Publishers: Dordrecht, The Netherlands, 1996; p 241.

(9) Fair, C. K. *MolEN, An Interactive Intelligent System for Crystal Structure Analysis*; Enraf-Nonius: Delft, The Netherlands, 1990.

(10) Sheldrick, G. M. *Acta Crystallogr. A* **1990**, *46*, 467.

(11) Sheldrick, G. M. *SHELXL97*; University of Göttingen: Göttingen, Germany, 1997.

result from diffraction on the uncorrelated iodine chains. Even if the chains have strong self-periodicity along the *a* axis, because they are not fixed relative to the donor lattice and hence not correlated with each other, the ensemble of chains would give the same diffraction pattern, that is, diffuse layer lines. The translation periods along *a* are equal to 4.10 and 3.27 Å for the donor and anion sublattices, respectively. The period of 4.10 Å corresponds to stacking periodicity of donor molecules along the *a* axis, and the period of 3.27 Å is characteristic of the mean value of the I−I distances in the chains. The ratio of the periods gives the compound composition as [ETEDT-TTF]$I_{1.254}$ or [ETEDT-TTF]$(I_3)_{0.42}$. This composition was also confirmed by EDX analysis. The observed ratio of the periods or the composition means that there could be commensurate structures with the formulas [ETEDT-TTF]$_5$-$(I_3)_2$ or [ETEDT-TTF]$_7(I_3)_3$ that are not realized because of the weak interaction of the iodine with the donor sublattice.

The intensities of the Bragg diffraction spots were collected with an Enraf Nonius CAD-4F diffractometer with Mo Kα radiation (graphite monochromator, ω-scan mode). Cell parameters and lattice symmetry were determined from both Weissenberg photographs and diffractometer data. All of the *hkl* reflections of orthorhombic lattice were of the type $h + k + l = 2n$, and no other reflection conditions were present. Thus, the probable space groups are *I*222, $I2_12_12_1$, *Imm*2, and *Immm*.

The ETEDT-TTF donor sublattice is considered to be the three-dimensional lattice that yields the diffraction spots. However, this does not mean that only the donor molecules contribute to the intensities of the reflections. Attempts to use traditional methods of crystal structure determination were not successful because of the strong disorder in a significant part of the structure, namely, the anion sublattice. Because of the ambiguity of the symmetry space group, we began a search of the crystal structure within noncentrosymmetric triclinic symmetry but still within a body-centered unit cell, to keep the same unit cell as for *Immm* lattice. Such a nonstandard space group could be denoted *I*1. In the Patterson synthesis analysis, we could conceive of a trial model structure consisting of the donor layers and the iodine chains. First, the assumption was made that the I chains make the main contribution to the 0*kl* reflections, and the projection of the full structure onto the (100) plane, that is, the two-dimensional pattern of the structure, was found. Then, the three-dimensional orientation of donor molecules was deduced by a comparison of the interatomic distances in the two-dimensional model with the expected molecular dimensions, and a trial structure consisting of four ETEDT-TTF molecules was found. The iodide ions were omitted at this stage. All of the 0*kl*-type reflections were omitted in the analysis of the ETEDT-TTF sublattice structure. The Fourier synthesis based on the atomic parameters of ETEDT-TTF exhibited nearly uniform, but nevertheless slightly modulated, columns of electron density running along the *a* axis. The columns were ascribed to the highly disordered triiodide anions. Further, iodine atoms were included in the model structure: they were placed on the electron density maxima of the columns. Analysis of the arrangement of the molecular moieties in the structure apparently showed that the space group must be *I*222. Finally, all non-hydrogen atoms of ETEDT-TTF and three disordered iodine atoms were refined within the *I*222 group of symmetry using all reflections by the full-matrix least-squares method.[12] The relatively large *R* value obtained for this refinement (0.078) is rather reasonable in view of the average structure and the significant disorder in the iodine channels.

For [ETEDT-TTF](I_yBr_{3-y}), X-ray data were collected at 213 K with a Bruker P4 diffractometer using monochromatic Mo Kα (λ = 0.710 73 Å) radiation via ω scans and corrected for Lorentz polarization. An empirical absorption correction based on Ψ scans was also applied. The structure was solved and refined with the Sheldrick program package. Atomic coordinates and other related structural data are provided as Supporting Information.

(12) Sheldrick, G. M. *SHELX93: Program for Refinement of Crystal Structures*; University of Göttingen: Göttingen, Germany, 1993.

EDX. The EDX analysis was performed with a Hitachi S-3000N scanning electron microscope (SEM) with an EDX-NORAN instrument.

Powder X-ray Diffraction Measurements. A Siemens 2000 diffractometer in the reflection $\theta-2\theta$ mode using Cu K(α_1) radiation was used.

Raman Spectroscopy. A Jobin-Yvon T64000 Micro-Raman spectrometer working in backscattering mode was used. The measurements were performed with the 633-nm laser line (458-nm laser line for BL films) and with spectral resolution of 1 cm^{-1}. The diamond (1332 cm^{-1}) line was used for the calibration of the spectrometer.

EPR Spectroscopy. EPR spectra at temperatures in the range of 4−300 K were obtained with an X-Band Bruker ESP 300E spectrometer equipped with a rectangular cavity operating in T102 mode, a Bruker variable-temperature unit, and an Oxford EPR-900 cryostat; a field frequency lock ER 033M system; and an NMR ER 035M gaussmeter. The modulation amplitude was kept well below the line width, and the microwave power was well below saturation.

Scanning Electronic Microscopy. The morphology of conducting surface layers was investigated using a scanning electron microscope (JEOL JSM-6300) operating at 20 kV.

Transport Properties. Temperature resistance dependencies were measured down to 1.5 K using a standard four-probe dc method. Four annealed platinum wires (20 μm in diameter) were attached to the conducting surface of a BL film by a conductive graphite paste.

Electronic Spectroscopy. Transmission measurements of finely ground KBr pellet samples (about 1 wt %) or of film samples were carried out with a Nicolet 5ZDX interferometer with Fourier transform (400−4400 cm^{-1}) and a Varian Cary 5 spectrometer (3330−20 000 cm^{-1}).

Band Structure Calculations. The tight-binding band structure calculations were based on the effective one-electron Hamiltonian of the extended Hückel method.[13] The off-diagonal matrix elements of the Hamiltonian were calculated according to the modified Wolfsberg−Helmholz formula.[14] All valence electrons were explicitly taken into account in the calculations, and the basis set consisted of single-ζ Slater-type orbitals for C 2s and 2p, S 3s and 3p, and H 1s. The exponents, contraction coefficients, and atomic parameters were taken from previous work.[15]

Results and Discussion

Synthesis of the Crystals. Crystals of ETEDT-TTF with trihalide anions were obtained electrochemically in conventional H-shaped cells (see Experimental Section). When PhCl was used as the solvent, only the completely ionic salts 1:1 were obtained, whereas when THF or CH_2Cl_2 was used, a mixture of crystals of the ionic and the mixed-valence salt was collected in the cell. This mixture of salts was also formed by direct chemical reaction between the donor and the halogens (I_2 or IBr) in CH_2Cl_2. Even though both salts were found to be ruler-shaped, the crystals from the mixed-valence salt could be discriminated from the completely ionic ones by their shinier and more polished surfaces. Because of the difficulty in obtaining pure phases, several techniques (vide infra) were used for the characterization of selected single crystals of the salts.

To determine the stoichiometry of the salts and also their composition, EDX measurements were carried out. From these analyses, the ETEDT-TTF salts were iden-

(13) Whangbo, M.-H.; Hoffmann, R., *J. Am. Chem. Soc.* **1978**, *100*, 6093.

(14) Ammeter, J.; Bürgi, H.-B.; Thibeault, J.; Hoffmann, R. *J. Am. Chem. Soc.* **1978**, *100*, 3686.

(15) Pénicaud, A.; Boubekeur, K.; Batail, P.; Canadell, E.; Auban-Senzier, P.; Jérome, D. *J. Am. Chem. Soc.* **1993**, *115*, 4101.

Table 1. X-ray, EDX, and Raman Data of Salts 1a−4a

		EDX data					
		analysis (atom %)				Raman data	
salt	X-ray data	S	I	Br	composition[a]	bands[b] (cm^{-1})	assignment
1a	$[ETEDT\text{-}TTF]I_3$	69.5	30.5	−	$[ETEDT\text{-}TTF](I_3)_{1.03}$	106.2	I_3^-
2a	$[ETEDT\text{-}TTF](I_3)_{0.42}$	84.5	15.5	−	$[ETEDT\text{-}TTF](I_3)_{0.43}$	107.3	I_3^-
3a	$[ETEDT\text{-}TTF](I_yBr_{3-y})$	69.5	25.0	5.5	$[ETEDT\text{-}TTF]\ I_{2.52}Br_{0.55}$	108.1 (i)	I_3^-
					or	145.6 (m)	I_2Br^-
					$[ETEDT\text{-}TTF](I_yBr_{3-y})_{1.02}$	179.6 (m)	IBr_2^-
4a	−	84.5	14.5	1.0	$[ETEDT\text{-}TTF]I_{1.20}Br_{0.08}$		
					or	104.4	I_3^-
					$[ETEDT\text{-}TTF](I_yBr_{3-y})_{0.43}$	107.7 (i)	I_3^-
$TBA(I_2Br)_y(I_3)_{1-y}$	−	−	−	−	−	127.4 (w)	I_2Br^-

[a] The exact composition of the type of anions forming salts **3a** and **4a** cannot be determined. To reach the formula shown above, we considered that the anions were always formed by three atoms: I_3^-, I_2Br^- or IBr_2^-. Thus, $[ETEDT\text{-}TTF]I_mBr_n$ can be expressed as $[ETEDT\text{-}TTF](I_yBr_{3-y})_{(m+n)/3}$. [b] i: intense; m: medium; w: weak.

Table 2. Crystal Data and Structure Determination Details for Salts 1a−3a

compound:	$[ETEDT\text{-}TTF]I_3$ **1a**	$[ETEDT\text{-}TTF](I_yBr_{3-y})$ **3a**	$[ETEDT\text{-}TTF](I_3)_{0.42}$ **2a**
formula	$C_{10}H_8S_7I_3$	$C_{10}H_8\ S7(I_3Br_{3-y})_3$[a]	$C_{10}H_8S_7I_{1.26}$
M	733.28	−	512.48
T (K)	293	213	293
crystal system	monoclinic	monoclinic	orthorhombic
space group	$P2_1/m$	$P2_1/m$	$I222$
a (Å)	12.978(3)	12.987(2)	4.0932(4)
b (Å)	9.303(1)	9.230(2)	10.980(2)
c (Å)	15.574(2)	15.326(2)	34.195(6)
α (°)	90	90	90
β (°)	95.41(1)	95.36(2)	90
γ (°)	90	90	90
V (Å^3)	1871.9(5)	1829.1(5)	1536.8(4)
Z	4	4	4
D_{calc} (g cm^{-3})	2.602	2.492	2.215
μ (cm^{-1})	57.77	64.08	35.36
ranges of h, k, l	$-18 \le h \le 18$	$0 \le h \le 12$	$0 \le h \le 4$
	$-13 \le k \le 0$	$-1 \le k \le 9$	$-13 \le k \le 13$
	$-22 \le l \le 0$	$-15 \le l \le 15$	$-40 \le l \le 40$
$2\theta_{max}$ (°)	60.82	40.98	50
reflns collected	5986	2255	2250
independent reflns	3168	1408	689
R	0.043	0.048	0.078
w$R2$	0.123	0.098	0.223
crystal size (mm^3)	0.31 × 0.20 × 0.06	0.20 × 0.10 × 0.045	0.38 × 0.08 × 0.04

[a] The crystallographic positions of the I and Br atoms cannot be differentiated.

tified as $[ETEDT\text{-}TTF](I_3)_{1.03}$ (**1a**), $[ETEDT\text{-}TTF](I_3)_{0.43}$ (**2a**), $[ETEDT\text{-}TTF]I_{2.52}Br_{0.55}$ (**3a**), and $[ETEDT\text{-}TTF]I_{1.20}Br_{0.08}$ (**4a**) (Table 1). These results are in agreement with the crystal structures described below for **1a**−**3a**. Unfortunately, crystals of the mixed-valence salt **4a** with good enough quality for X-ray determination were not obtained. However, by EDX, it was possible to determine their stoichiometry, which was found to be the same as that obtained for the salt with iodine **2a**. EDX is also a useful tool for determining the anion composition, in particular, in the molecular solids prepared from $TBA(I_2Br)_y(I_3)_{1-y}$, as it can identify different trihalide anions. It is worth noting that, whereas in the mixed-valence salt **4a** iodine is the main counterion, in the completely ionic salt **3a**, there is a considerable proportion of bromine. These remarks about the anion composition in these salts will be further discussed below, together with the Raman results.

X-ray Single-Crystal Structure. Molecular and crystalline structure analysis was performed for **1a**, **2a**, and **3a** by single-crystal X-ray diffraction. The stoichiometries found for these salts are $[ETEDT\text{-}TTF]I_3$, $[ETEDT\text{-}TTF](I_3)_{0.42}$, and $[ETEDT\text{-}TTF](I_yBr_{3-y})$, respectively. The crystallographic parameters are given in Table 2. The two completely ionic salts, **1a** and **3a**, are isostructural. In both structures there is 50% disorder of the ethylenethio groups and also disorder of the ethylene groups of the six-membered ring, with two possible positions, C1(up)−C2(down) and C1(down)−C2(up), in relation to the S−C−C−S plane. The molecular structures and the corresponding atomic numbering are shown in Figure 1a. The asymmetric unit of the crystal contains two half-molecules of the donor perpendicular to a crystallographic mirror plane and two anions in special positions of the mirror plane with occupancy of 0.5 each. Similarly to the neutral donor,[4] the TTF cores in these salts deviate significantly from planarity. In both completely ionic salts, the donor molecules form strong dimers having the molecules in the same orientation, although for the neighboring dimers, the orientation is head-to-tail (Figure 1b). The intermolecular distance in the dimers is 3.317 Å for the salt with I_3^- and 3.310 Å for the salt with $(I_yBr_{3-y})^-$. These dimers form layers in the *bc* plane that are separated along *a* by the molecules of the anions that are perpendicular to the donors. Considering each layer, the dimers form not stacks but, rather, a 2D network

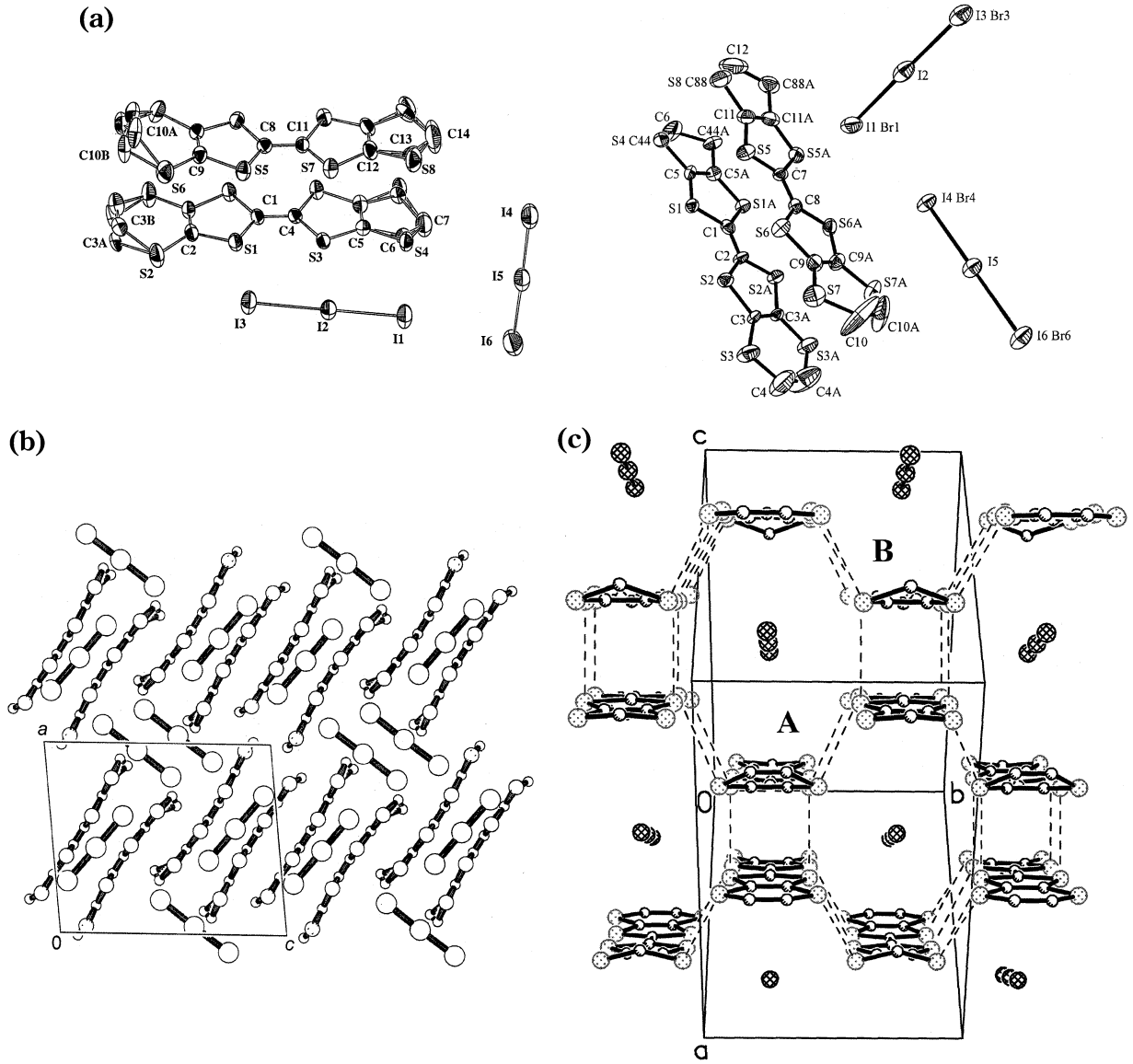

Figure 1. (a) Molecular structures of [ETEDT-TTF]I_3 (**1a**) and [ETEDT-TTF](I_yBr_{3-y}) (**3a**). (b) Projection of the crystal packing perpendicular to the *ac* plane of the salt **3a**. (c) View of a donor layer showing the short inter- and intradimer contacts.

Table 3. S···S Short Distances in the [ETEDT-TTF]I_3 and [ETEDT-TTF](I_yBr_{3-y}) Salts

distances S···S (Å)	N^a	[ETEDT-TTF]I_3 **1a**	[ETEDT-TTF](I_yBr_{3-y}) **3a**
intradimer	7	3.333−3.879	3.317−3.799
interdimer A	3	3.567−3.986	3.518−3.959
interdimer B	5	3.521−3.643	3.517−3.611
interlayer	1	3.529	3.525

[a] Number of contacts per molecule.

with holes in which the anions parallel to the ETEDT-TTF molecules are located (Figure 1c). There are also short S···S intra- and interdimer contacts forming a bidimensional network (Figure 1c, Table 3). As shown in Figure 1c, there are two kinds of interdimer interactions (A and B), because the dimers inside the unit cell are shifted along the longest axis of the molecules. Short S···S contacts (3.529 Å) between the layers can also be observed between the sulfur atoms of the five-membered rings, which can be interrupted by the disorder.

Figure 2a shows the crystal structure of **2a** viewed along the *a* axis. The structure is characterized by ETEDT-TTF radical cation layers alternating with anion layers along the *c* direction. The projection of the radical cation layer along the long molecular *a* axis is shown in Figure 2b. It is a θ-type layer in which the molecular planes of the adjacent stacks are tilted alternately in the opposite directions (Figure 2b). The dihedral angle between the planes of the neighboring molecules interrelated by the screw-axis symmetry is 45.8°. The cation layer is built from regular ETEDT-TTF stacks parallel to the short *a* axis. The overlap mode of adjacent radical cations in the stack is shown in Figure 2c. The mean donor interplanar distances in stack is 3.723 Å. There are several short S···S interstack contacts of 3.567−3.557 Å. Thus, the **2a** salt is two-dimensional in crystal structure and semiconducting. It should be noted that the crystal structure of the radical cation salt [ETEDT-TTF]$(I_3)_{0.42}$ [or [ETEDT-TTF]$_{2.4}I_3$] appears to be intermediate between the organic superconductor θ-(BEDT-TTF)$_2I_3$[16] and organic metal β''-(BEDO-TTF)$_{2.4}I_3$.[17] As a rule, the planes of the radical cations from neighboring stacks are approxi-

(16) Kobayashi, H.; Kato, R.; Kobatashi, A.; Nishio, X.; Kajita, K.; Sasaki, W. *Chem. Lett.* **1986**, *789*, 833.

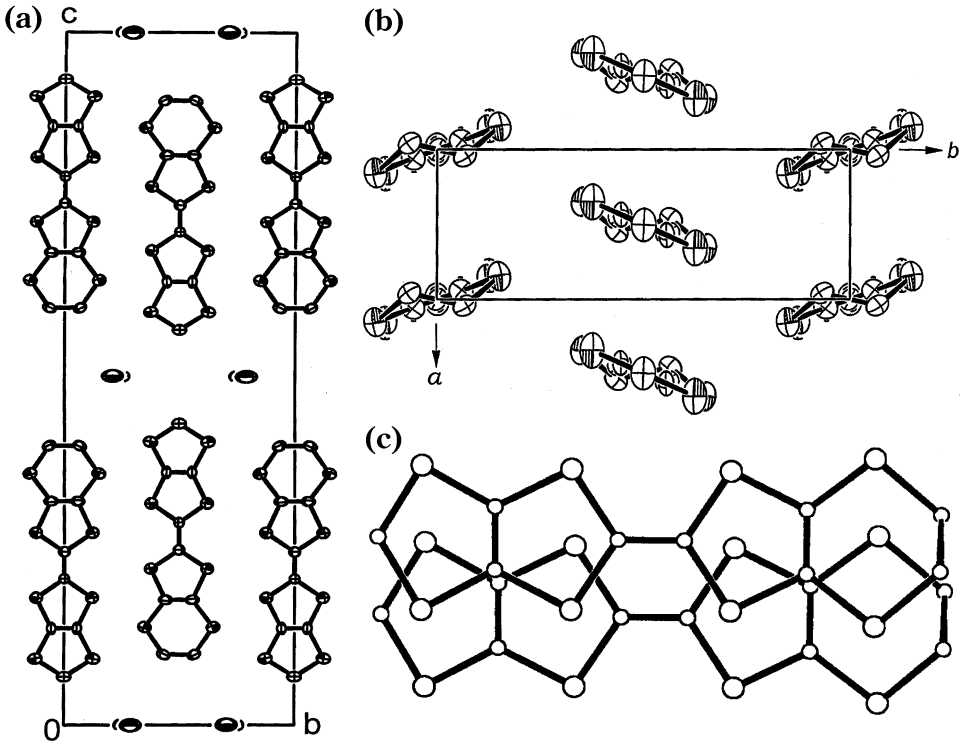

Figure 2. (a) Projection of the crystal structure [ETEDT-TTF]$(I_3)_{0.42}$ (**2a**) along the *a* direction. (b) Projection of the radical cation layer along the *c* direction. (c) Mode of radical cation overlap in the stacks.

mately perpendicular to each other in θ-type organic metals, and radical cation stacks run along the period close to 5 Å.[18] However, in β'' salts, all radical cations are parallel to each other, and the radical cation stacks have a period close to 4 Å.[19]

Optical Properties and Determination of the Anion Composition. The mixed-valence character of the [ETEDT-TTF]$(I_3)_{0.42}$ (**2a**) and [ETEDT-TTF]-$(I_yBr_{3-y})_{0.42}$ (**4a**) salts was confirmed by the presence of the characteristic broad A band in the IR and vis/NIR spectra, centered at 3040 nm, corresponding to the mixed-valence states of low-dimensional conducting organic solids (Figure 3).[20] These salts also exhibit a B band at ca. 840 nm, whereas the ionic salts **1a** and **3a** present only the B band at around 1128 and 955 nm, respectively, as expected from their ionic nature.

Low-frequency Raman measurements were performed because Raman spectroscopy has previously been demonstrated to be a very useful technique for determining the types of trihalide anions included in crystal structures.[21] As expected, **1a** and **2a** exhibit only the bands corresponding to the stretching vibration of the I_3^- trihalide (Table 1). Of much interest is the study of the composition of the salts obtained from TBA$(I_2Br)_y(I_3)_{1-y}$, as they can contain a mixture of anions. In the Raman spectra of this starting salt, two bands due to the I_3^- and I_2Br^- anions were observed. On the other hand, in the mixed-valence salt **4a**, we found only the vibration bands of I_3^-, whereas, in the ionic salt **3a**, the stretching bands coming from I_3^-, I_2Br^-, and IBr_2^- were observed (Table 1). In both compounds, iodine is the major component. All of these results are in accordance with the EDX data, as bromine was hardly detected for **4a** (Table 1).

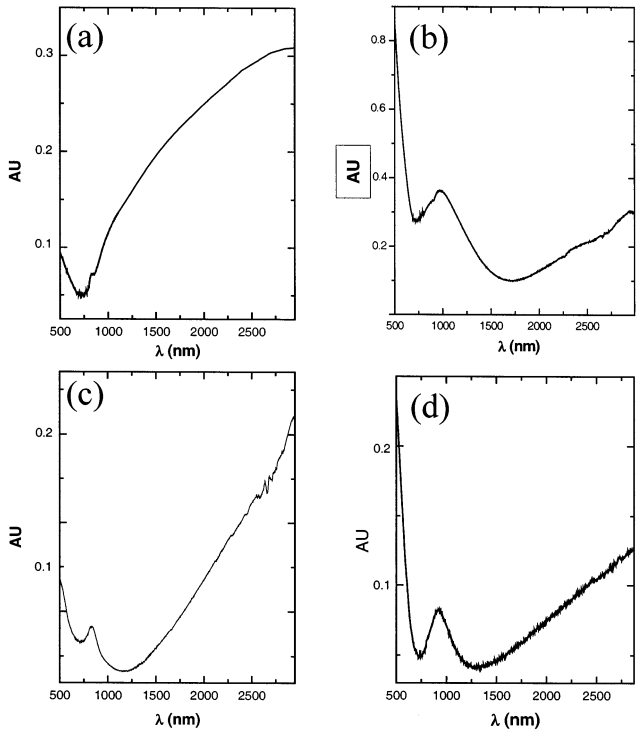

Figure 3. Vis−NIR spectra of (a) **2a**, (b) **4a**, (c) **2b**, and (d) **4b**.

(17) (a) Wudl, F.; Yamochi, H.; Suzuki, T.; Isotalo, H.; Fite, C.; Kasmai, H.; Liou, K.; Srdanov, G.; Coppens, P.; Maly, K.; Frost-Yensen, A. *J. Am. Chem. Soc.* **1990**, *112*, 2461. (b) Petrichek, V.; Maly, K.; Coppens, P.; Bu, X.; Cisarova, I.; Frost-Yensen, A. *Acta Crystallogr. Sec. A*, **1991**, *47*, 210.

(18) Mori, T.; Mori, H.; Tanaka, S. *Bull. Chem. Soc. Jpn.* **1999**, *72*, 179.

(19) Mori, T. *Bull. Chem. Soc. Jpn.* **1998**, *71*, 2509.

(20) Torrance, J. B.; Scott, B. W.; Kaufman, F. B.; Seiden, P. E. *Phys. Rev. B* **1979**, *19*, 730.

(21) (a) Wojciechowski, R.; Ulanski, J.; Lefrant, S.; Faulques, E.; Laukhina, E.; Tkacheva, V. *J. Chem. Phys.* **2000**, *112*, 7634. (b) Sugai S.; Saito, G. *Solid State Commun.* **1986**, *58*, 759.

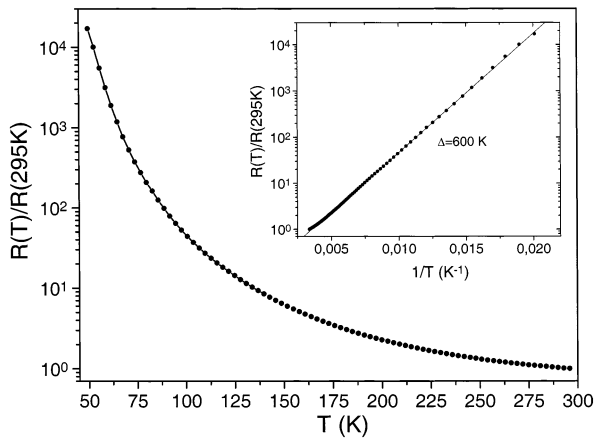

Figure 4. Temperature dependence of the normalized resistance for the salt **2a**. The inset shows a semilogarithmic plot of the same dependence.

Transport Properties. As expected, the room-temperature conductivity values of the completely ionic salts [ETEDT-TTF]I_3 and [ETEDT-TTF](I_yBr_{3-y}) are lower than 10^{-5} S·cm^{-1}, demonstrating their dielectric behavior. This is in accordance with the EPR results shown below and indicates that the electrons of [(ETEDT-TTF)$^{\bullet+}$]$_2$ are localized and antiferromagnetically coupled, a result that is reasonable considering the low intradimer distances. In contrast, the mixed-valence salt [ETEDT-TTF]$(I_3)_{0.42}$ displays a high room-temperature conductivity of 24 S·cm^{-1} and reveals semiconducting transport properties with an activation energy of 600 K (Figure 4).

Band Structure. The donor layers of [ETEDT-TTF]-$(I_3)_{0.42}$ have the typical θ-type packing, and the salt exhibits semiconducting behavior but high room-temperature conductivity. To gain some insight into the correlation between the crystal structure and the transport properties of this salt, we carried out tight-binding band structure calculations. Because of the disorder in the donor layers, the calculations were carried out for (a) a fully ordered layer (i.e., a donor layer without rotational disorder, which is the layer with the more uniform distribution of intermolecular S···S contacts) and (b) a layer in which the five-membered rings were substituted by two hydrogens and all other geometrical details were left unaltered (i.e., using EDT-TTF molecules with the same geometry so that the effects of the sulfur atoms affected by the disorder were completely removed). These models should give upper and lower bounds for the band dispersion. The calculated band structure and Fermi surface assuming metallic filling of the bands for the fully ordered layer are shown in Figure 5. Both the band structure and the Fermi surface are the typical of θ-type phases.[22a] The total bandwidths and the Fermi surfaces calculated for layers a and b are practically identical, so that disorder does not have a noticeable effect in the topology of the band structure and Fermi surface, although it can still influence the transport properties of the salt. The total bandwidth is 0.53 eV, which, in fact, is considerably smaller than the values in the series of metallic $(ETEDT\text{-}TTF)_2XF_6$ (X = P, As, Sb) salts,[23] where the total bandwidth of the two overlapping bands is 0.8−0.9 eV. Although this is the only series of metallic salts of the ETEDT-TTF donor and thus the comparison should be taken with caution, the simultaneous occurrence of a comparatively small bandwidth *and* disorder makes understandable the semiconducting behavior of this salt.

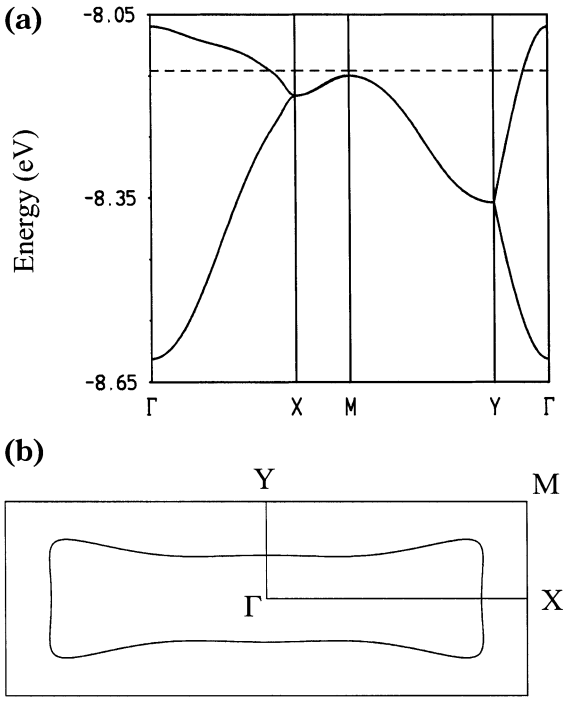

Figure 5. (a) Band structure and (b) Fermi surface calculated for the donor lattice of [ETEDT-TTF]$(I_3)_{0.42}$ assuming an ordered distribution of donors. The dashed line in a indicates the Fermi level assuming metallic filling of the bands and Γ = (0, 0), X = (a*/2, 0), Y = (0, b*/2), and M = (a*/2, b*/2).

At this point it is useful to recall the work of Mori et al.[22] on the metallic vs semiconducting behavior of BEDT-TTF and BEDT-TSF θ-type salts. They proposed that there is a relationship between the metal−insulator transition temperature and the angle between the planes of the two donors in neighboring stacks. They showed that the metal−insulator transition temperature is controlled by this angle simply because the transfer integral, and consequently the bandwidth, increases when the angle decreases. Thus, for BEDT-TTF salts, when the angle is larger than 120°, the salts are semiconductors at room temperature, but if the angle is smaller, the transition temperature decreases when the angle decreases. In other words, the metallic state is more stable when the angle decreases. For BEDT-TSF salts, where the ratio between "on-site" Coulombic repulsion and bandwidth (U/W) decreases, the metallic state is stable for even higher angles. In the case of ETEDT-TTF, because a sulfur atom is missing with respect to BEDT-TTF, U should be larger and W smaller so that the ratio U/W should be larger. In conclusion, according to the Mori et al. scheme, the metallic state of θ-type salts of ETEDT-TTF should be stable only for angles smaller than those of the BEDT-TTF salts. Because the BEDT-TTF salts are room-

(22) (a) Mori, T., Mori, H.; Tanaka, S., *Bull. Chem. Soc. Jpn.* **1999**, *72*, 179. (b) Mori, H.; Sakurai, N.; Tanaka, S.; Moriyama, H.; Mori, T.; Kobayashi, H.; Kobayashi, A. *Chem. Mater.* **2000**, *12*, 2984.

(23) Laukhin, V.; Ribera, E.; Rovira, C.; Veciana, J.; Gener, M.; Canadell, E.; Togonidze, T.; Khasanov, S. S.; Shibaeva, R.; Biberacher, W., Andres, K.; Kartsovnik, M. V. *Synth. Met.* **1999**, *102*, 1772.

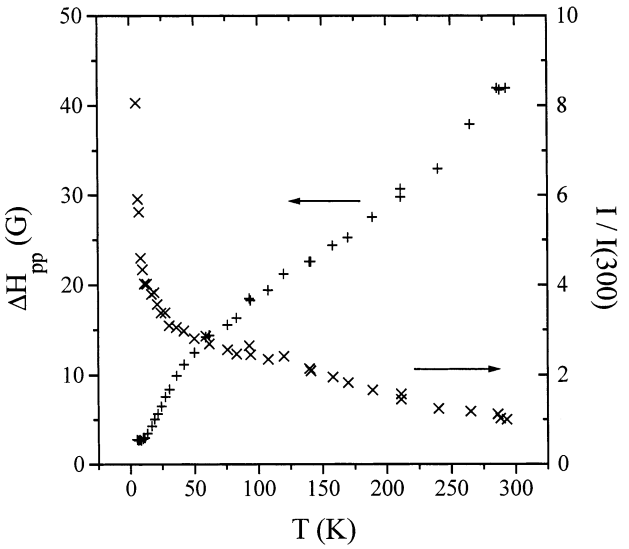

Figure 6. Temperature dependence of EPR parameters (signal intensity and line width) for **2a**.

Table 4. EPR Data of the BL Films Based on ETEDT-TTF

	parallel[a]		perpendicular[b]	
film	*g* factor	line width (G)	*g* factor	line width (G)
ETEDT-TTF + I_2 **2b**	2.0047	42	2.0084	65
ETEDT-TTF + IBr **4b**	2.0047	42	2.0090	57

[a] Field parallel to film. [b] Field perpendicular to film.

temperature semiconductors for angles of 120° or larger,[22] it is expected that, for ETEDT-TTF salts, the metallic state could be stable at room temperature only for angles smaller than 120°. In the present case, however, this angle is 134°! Thus, even without taking into account the existence of disorder, it is clear that [ETEDT-TTF]$(I_3)_{0.42}$ must be a room-temperature semiconductor and that it fits into the general scheme proposed by Mori et al. for θ-type phases.

Electron Paramagnetic Resonance. The ionic salts [ETEDT-TTF]I_3 and [ETEDT-TTF](I_yBr_{3-y}) do not display any EPR signal in the range 4−300 K, indicating that there are no unpaired electrons because of the above-mentioned antiferromagnetic coupling. However, the mixed-valence salt [ETEDT-TTF]$(I_3)_{0.42}$ exhibits an EPR signal with *g* values typical of the organic donor. The study of the dependence of the EPR parameters with temperature fits with its semiconductor properties. As shown in Figure 6, with decreasing temperature, the signal intensity increases progressively, and a decrease of the line width begins. Such behavior is characteristic of systems with localized electrons. Below 50 K, a magnetic transition can also be observed, but it has not yet been further investigated. The *g* factor and the line width (in parentheses) in the three directions of a single crystal of **2a** were found to be 2.0086 (64 G), 2.0060 (44 G), and 2.0022 (41 G).

Conducting Bilayered Films. Our successful achievement of crystals based on ETEDT-TTF and trihalide anions exhibiting high room-temperature conductivity prompted us to prepare BL films.[7] The aim in preparing these films was to produce a processible material with high potential applications achieving the same transport properties as the single crystals. Moreover, the fact that the mixed-valence crystals **2a** and **4a** were obtained not only electrochemically but also by direct reaction was an encouraging point for the potential production of BL conducting surface films.

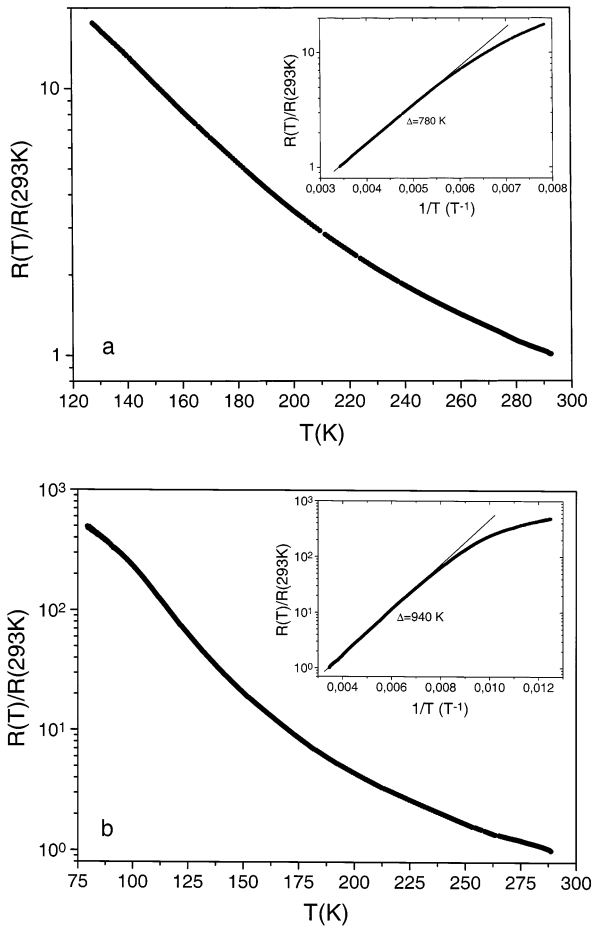

Figure 7. Temperature dependence of the normalized resistance for the BL films (a) **2b** and (b) **4b**. The insets show semilogarithmic plots of the same dependence.

Following the described methods for the preparation of BL films and using solutions of I_2 and IBr in CH_2Cl_2, two different sets of films, namely, **2b** and **4b**, respectively, were obtained (see Experimental Section). These films have the same physical characteristics (flexibility, low density and transparency) as those that have been previously reported.[6,7] Their vis−NIR spectra are very similar to those of the single crystals **2a** and **4a**, including the characteristic broad A band for partially ionized systems and also the B band (Figure 3). To confirm the formation of the mixed-valence salts, EPR spectra of the films were recorded with the static magnetic field oriented parallel and perpendicular to the films, displaying a signal arising from the unpaired electron centered on the TTF core (Table 4). It is worth mentioning that the signal observed when the magnetic field was perpendicular to the film **2b** had the same EPR parameters as the signal from one of the directions of a single crystal of **2a**. In contrast, when the field was parallel to the film, the EPR parameters had averaged values of the parameters corresponding to the other two directions of the crystals **2a**. These results imply that oriented nanocrystals of the same θ phase might have been formed on the film surface. Furthermore, we draw attention to the fact that the EPR parameters are

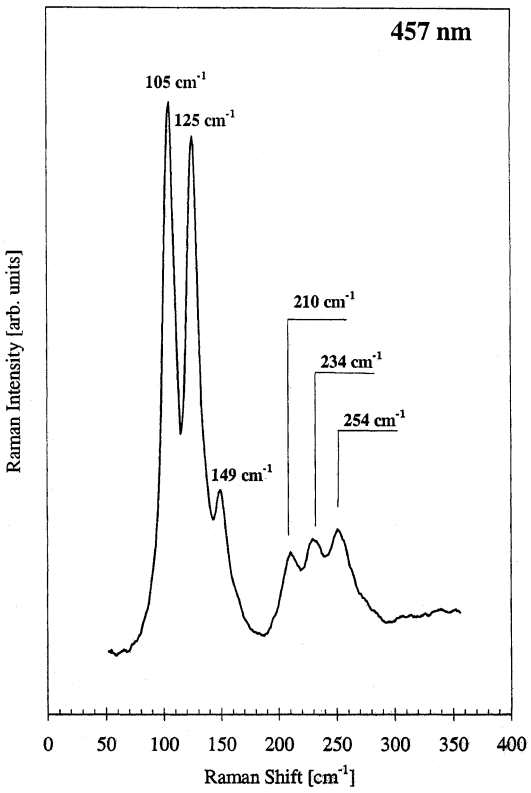

Figure 8. Low-dimensional Raman spectrum of the BL film **4b**.

almost the same for the two films, indicating again that the nanocrystals on their surfaces are isostructural.

The σ_{293K} values of the films **2b** and **4b** were 0.25 and 2.5 S·cm^{-1}, respectively, which represents notable conductivity for this kind of material. The temperature dependence of the resistance of the BL films was measured down to 125 K and found to exhibit the same semiconducting behavior as observed for the mixed-valence salt with iodine **2a** (Figure 7). Thus, the transport properties of a new family of conducting organic salts have been successfully transferred to polymeric composite BL films.

In Figure 8, the low-frequency Raman spectrum of the BL film **4b** is shown. It contains the set of bands due to the vibrations of the trihalide anions I_3^- (105 cm^{-1}), I_2Br^- (125 cm^{-1}), and IBr_2^- (149 cm^{-1}) and their corresponding overtones. In contrast to the single crystals **4a** in which the counterions were composed basically by iodine, in the nanocrystals of the film sample **4b**, there is a considerable amount of bromine. It should also be added that the frequencies where the trihalide anions appear differ between the crystals and the films. This discrepancy might be due to the different orientations and local environments of the crystals.

As it was previously shown that the measured values of the interplanar spacing d_{001} along with the intensities of the (00*l*) reflections allow the different phases of the BEDT-TTF trihalides to be identified,[6b] we studied here the diffraction profiles of the film **2b** to verify the types of nanocrystals that form the conducting surface layer. The X-ray diffraction profiles of film samples indicate the presence of only (00*l*) reflections, which are characteristic of conducting layers formed by highly oriented nanocrystals. The crystallographic *c** axis of the nanocrystals is perpendicular to the film surface, and consequently, their conducting layers are parallel to the surface. The measured values of the interplanar spacing *d*(002) and the relative intensity of the lines of the

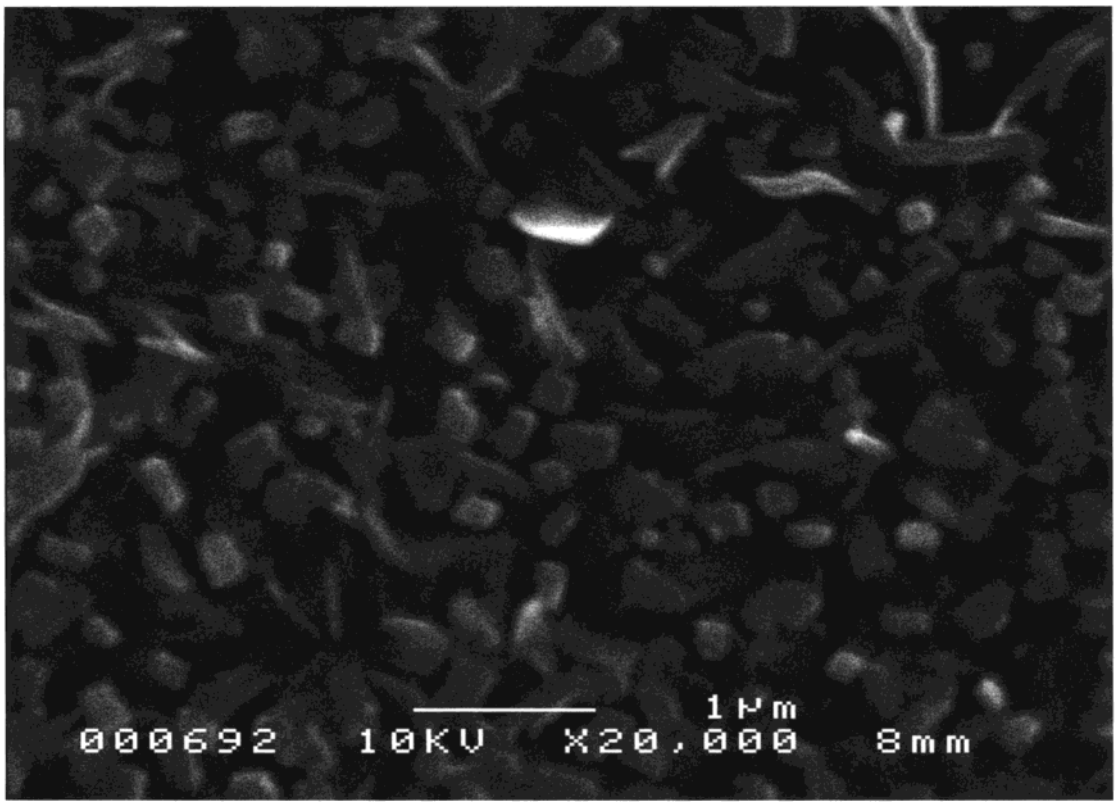

Figure 9. SEM images of the BL film **4b** exhibiting the conducting surface layer containing a network of interpenetrating nanocrystals.

nanocrystal for **2b** film samples correspond to the same phase as the single crystals of θ-(ETEDT-TTF)$_{0.42}$I$_3$ [$d(002) = 17.14(1)$ Å]. Unfortunately, because of sample decomposition caused by the X-ray irradiation, the X-ray data obtained for film samples **4b** were not good enough to permit characterization of the type of nanocrystals that form the conducting layer. Nevertheless, regarding the striking similarities of the EPR signals and the transport properties of the films **2b** and **4b**, it seems that the nanocrystals on the surface of **4b** are from the same θ-type phase as those of **2b**.

As the quality, orientation and contacts between the nanocrystals (200−300 nm) forming the conducting layer of the BL films were found to have a great influence on the film transport properties, the morphology of the conducting surface of the film samples was also studied by SEM. According to the SEM images, all film samples contain oriented crystals with nanoscopic dimensions (200−300 nm) that have their largest face (*bc* plane) parallel to the film surface. This is in agreement with the results obtained from the X-ray diffraction profiles. As an example, in Figure 9, we show the SEM images of the film sample **4b**, in which it can be seen that a nanocrystalline network covers the entire film surface, providing good contacts and, therefore, allowing good conductivity along the surface.

Conclusions

A new family of charge-transfer salts based on ET-EDT-TTF and trihalide anions has been synthesized and characterized. Interestingly, the mixed-valence salt **2a** displays semiconductor behavior and high room-temperature conductivity, which make it very attractive as a base component for the conducting layer of bilayer composite films. The large angle between the molecular planes of the two donors in salt **2a** precludes the possible metallic properties of this salt. By both electrochemical synthesis and direct chemical reactions, the conducting salts **2a** and **4a** were obtained mixed with the corresponding ionic insulators salts **1a** and **3a**. Good conditions for the preparation of conducting BL films containing only the mixed-valence phases were found. In accordance with their composition, the BL films display the same transport properties as the single crystals while also gaining the advantageous properties of polymeric matrixes such as flexibility, transparency, and low density. Undoubtedly, this success in the preparation of BL films with the physical properties of crystalline organic conductors is a step forward in the search for potential applications.

Supporting Information Available: Atomic coordinates and other related structural data. This material is available free of charge via the Internet at http://pubs.acs.org.

Acknowledgment. This work was supported by NATO (Project CRG.LG.974316), by DGI-Spain (BQU-2000-1157 and BFM2000-1312-C02-01), by Generalitat de Catalunya (2000 SGR-00114 and 1999 SGR-207), and by the Russian National Program "Physics of Quantum and Wave Processes", as well as by KBN (Poland) Grant 7 T08A 013 20. M.M.T. is grateful to Generalitat de Catalunya for a predoctoral grant. E.L. is grateful to Spanish Ministerio de Educacion y Cultura for a sabbatical at ICMAB (CSIC) and to the NATO Science Committee for a DC type grant.

CM021123G